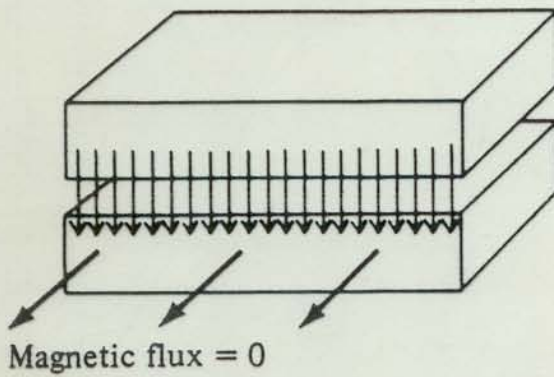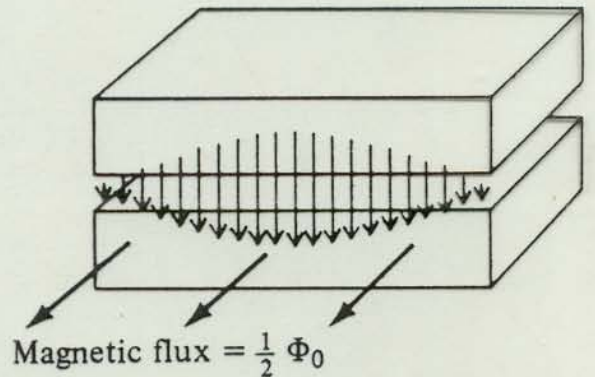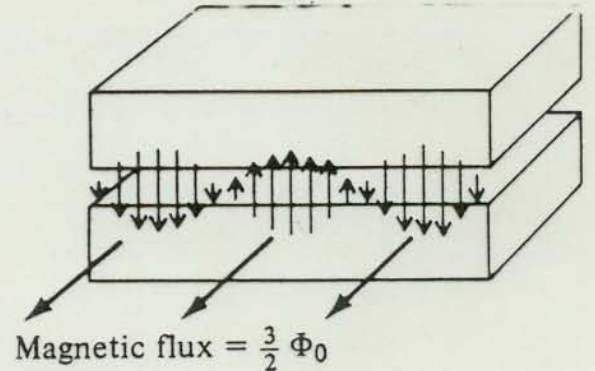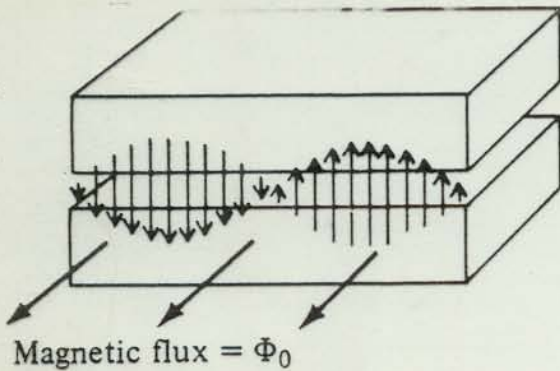**Figure 4.05d.** Dependence of the maximum zero-voltage current in a junction with a current density of the form in Fig. 4.05c as a function of the flux linking the junction.

Magnetic flux = 0

(i)

Magnetic flux = $\frac{1}{2}\Phi_0$

(ii)

Magnetic flux = Φ_0

Magnetic flux = $\frac{3}{2}\Phi_0$

parallel to the surface, and the distance z_0 between the surface and the pickup loop is typically a few micrometers. Although z_0 is known approximately from the experimental setup, in practice the exact value of z_0 at low temperatures should be considered an unknown. We detect the change in the flux through the pickup loop while scanning the sample in x and y, so that the signal for each data set has an arbitrary constant offset. When the 8.2-μm pickup loop is used to image an anisotropic vortex in Tl-2201 (Fig. 1A), the interlayer spacing, $s = 11.6$ Å, and the a-axis penetration depth, $\lambda_a = 0.17$ μm (15), are both smaller than the spatial resolution. The interlayer penetration depth λ_c corresponds to currents flowing between the layers (along the c axis).

We have previously imaged vortices in niobium films (14) and ab-plane vortices in YBa$_2$Cu$_3$O$_{7-\delta}$ (YBCO) films (12) and crystals (16). In these cases, the relevant penetration depths are much smaller than the size of the pickup loop, so the vortices are well approximated by monopole sources of magnetic flux (17, 18). Figure 1B shows images of two ab-plane vortices in YBCO, whose apparent shapes are determined by the shape of the pickup loop (19). In contrast, the interlayer vortices observed in images of the ac face of Tl-2201 (Fig. 1C) extend a considerable distance along the layers.

The Tl-2201 crystals were grown under carefully controlled conditions (20). The crystals we chose for these experiments were platelet-shaped, with a basal plane area of ~1 mm^2 and a thickness along the c axis varying between 50 and 100 μm. The images were made in a magnetically shielded dewar with an unknown residual field of several milligauss. We observed many similar ac-plane vortices in different parts of the two crystals. Five vortices (Fig. 1C) were chosen for detailed analysis because of their relatively large spacing from neighboring vortices. The vortices extend a few tens of micrometers along the a axis, indicating qualitatively that λ_c is a few tens of micrometers. The full width at half-maximum (FWHM) along the a axis ranged from 35 to 46 μm (Fig. 2).

Neglecting the influence of the surface on the fields, and defining a and c as the directions parallel and perpendicular to the layers, respectively, the z-component of the magnetic field of an interlayer Josephson vortex is given by

$$b_z(x_c, y_a, z = 0) = \frac{\Phi_0}{2\pi\lambda_a\lambda_c} K_0(\tilde{R}) \quad (3)$$

(10), where

$$\tilde{R} = [(s/2\lambda_a)^2 + (x_c/\lambda a)^2 + (y_a/\lambda c)^2]^{1/2} \quad (4)$$

K_0 is a modified Bessel function of the second kind (of order 0), and x_c and y_a denote the distance along the c axis and a axis, respectively (11). In our images, the crystal axes are rotated by 9° from the scan axes (Fig. 1). For these experiments, $\lambda_a \ll (L, \lambda_c)$, so it is appropriate to integrate over x_c at the surface. After this integration, the FWHM along y_a is $\sqrt{2}\lambda_c$. For

Fig. 1. (A) Sketch of an 8.2 μm by 8.2 μm pickup loop with shielded leads, together with a sketch of the magnetic fields of a highly anisotropic vortex. The flux through the pickup loop is given by the magnetic field B_z at a height $z_0 \approx 3$ μm, integrated over the area of the pickup loop; a and c indicate the Tl$_2$Ba$_2$CuO$_{6+\delta}$ crystal axes. The extent of the vortex along the a axis is called the c axis or interlayer penetration depth, because it is determined by supercurrents flowing between the layers, parallel to c. (B) For comparison, images of two YBa$_2$Cu$_3$O$_{6.95}$ ab-plane vortices. Because these vortices are much smaller than 8.2 μm, their apparent shape is dominated by the shape of the pickup loop. (C) Images of Tl$_2$Ba$_2$CuO$_{6+\delta}$ ac-plane vortices. Vortices I, II, and III were observed in crystal 1; vortices IV and V were observed in crystal 2. The vortices are resolution-limited in the c direction but extend tens of micrometers along the a axis, indicating qualitatively that λ_c is a few tens of micrometers.

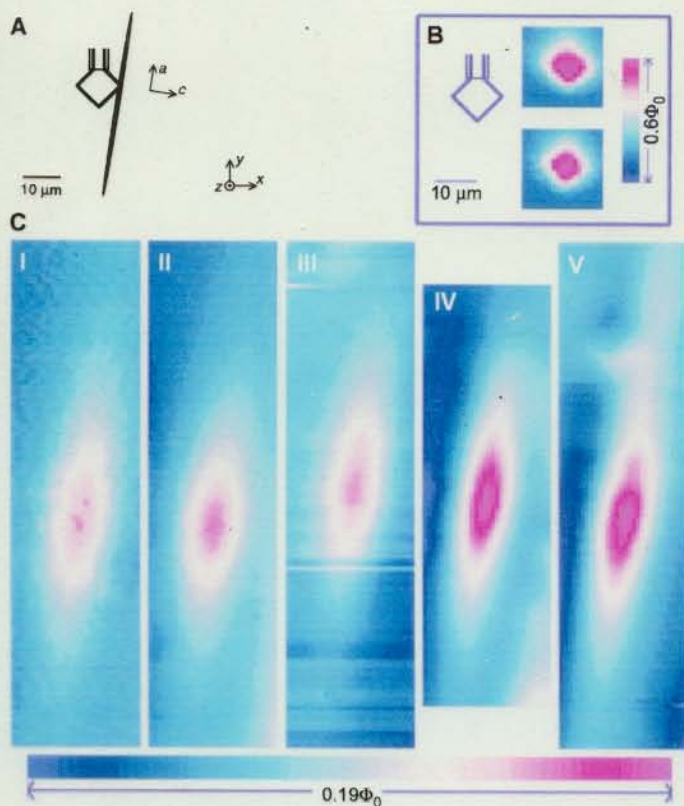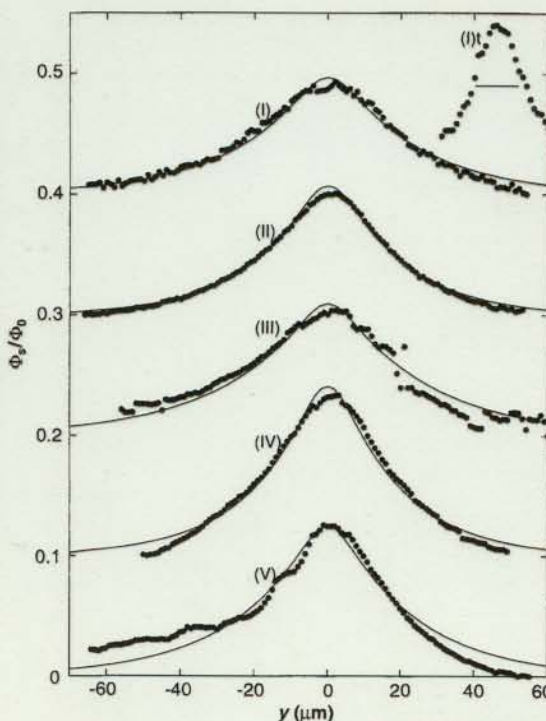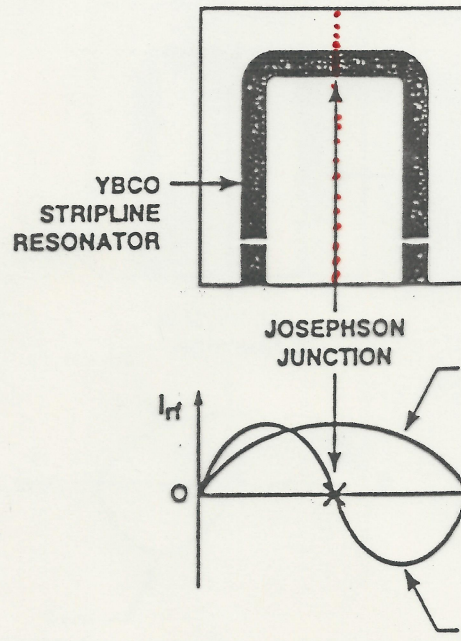**Fig. 2.** Longitudinal cross sections along the a axis through the vortices from Fig. 1, plotted as the flux through the SQUID pickup loop, Φ_s (offset in 0.1Φ_0 increments) versus y. The data are fit to the functional form for the magnetic fields of an interlayer Josephson vortex with interlayer penetration depth λ_c, propagated to the height of the pickup loop above the surface, z_0, and integrated over the pickup loop. The fit parameters are: (I) $\lambda_c = 22^{+6}_{-4}$ μm, $z_0 = 3.0 \pm 0.6$ μm; (II) $\lambda_c = 18 \pm 2$ μm, $z_0 = 3.4 \pm 0.4$ μm; (III) $\lambda_c = 25^{+10}_{-7}$ μm, $z_0 = 2.0 \pm 1.0$ μm; (IV) $\lambda_c = 18 \pm 3$ μm, $z_0 = 2.2 \pm 0.6$ μm; and (V) $\lambda_c = 22^{+11}_{-7}$ μm, $z_0 = 1.9 \pm 1.0$ μm. A transverse cross section along x is also shown, with a scale bar indicating the extent of the pickup loop along x, 11.6 μm. The weighted average of the penetration depths is $\lambda_c = 19 \pm 2$ μm.

Bi-Crystal Substrate

YBCO STRIPLINE RESONATOR

JOSEPHSON JUNCTION

Dan Oates
PRB 57, 13833
(1998)

I_{rf}

n = 1

O

y

L

n = 2

Change in Inductive Microwave Loss

10^{-3} $1/Q$

10^{-3} $\Delta f/f_n$

(a)

n = 1

1

n = 2

0.1

(b)

0.15

n = 1

0.05

n = 2

0.0001   0.001   0.01   0.1   1

I_{rf} (A)

I_1 I_2 I_3 I_4

L_l L_l L_l ... etc.

JJ R_n JJ R_n JJ R_n JJ R_n

L_l L_l L_l ... etc.

I_1 I_2 I_3 I_4